FINITE ELEMENT MODELING OF THE RTM PROCESS

Z. Dimitrovová and L. Faria

IDMEC, Department of Mechanical Engineering, Instituto Superior Técnico,
Av. Rovisco Pais 1, 1096 Lisbon, Portugal
(zdimitro@dem.ist.utl.pt and Luis.Faria@lemac-pt.com)

ABSTRACT

Some new aspects are introduced into the numerical simulation of the mold filling phase of the Resin Transfer Molding process of composites manufacturing. The problem formulation is based on homogenization techniques. On the microlevel, the well-known analogy is exploited in order to determine the permeability tensor. The suitability of the cell-averaged permeability and of solving the macrolevel problem on two levels is addressed in the case of the double porosity problem. An algorithm allowing the determination of the progression of the resin front on the microlevel is developed. Regarding the macrolevel analysis, a new approach based on an analogous problem is proposed and determination of the resin front position in multiple-layer preforms is presented. Results are obtained by the finite element code ANSYS.

1 INTRODUCTION

The Resin Transfer Molding (RTM) process has recently become one of the most important processes of fiber reinforced composites manufacturing. The process consists of three phases: an arrangement of fiber mats in a mold cavity, a mold filling by a polymeric resin and a curing phase. Due to the large number of fibers and very low ratio of their characteristic cross-sectional size to the size of the mold, direct numerical solution of the filling-phase problem is almost impossible. Homogenization techniques are often used in order to reformulate the original problem in terms of the microlevel (local) and the macrolevel (global, effective) analyses. If restriction to the isothermal case is adopted, the resin flow can be viewed as slow flow of an incompressible isotropic Newtonian liquid with high viscosity and constant properties. In this case the microlevel and macrolevel analyses have forms allowing finding problems analogous with them, which are included in many general-purpose commercial finite element (FE) codes, e.g. in ANSYS ([1-3]).

2 HOMOGENIZATION TECHNIQUES

Governing equations of the filling phase problem under the assumptions specified above are ([4]):

$$\nabla \cdot \mathbf{v} = 0 \text{ and } \rho \frac{\partial \mathbf{v}}{\partial t} = -\nabla p + \mu \Delta \mathbf{v} + \mathbf{F}, \tag{1}$$

where $\mathbf{v}$, t, p, $\mathbf{F}$ stand for the velocity vector, time, pressure and the volume force vector, respectively; ρ and μ are the resin density and the coefficient of the resin viscosity. As usual $\nabla = \{\partial/\partial x_1, \partial/\partial x_2, \partial/\partial x_3\}$, $\mathbf{x}$ is the spatial variable, $\Delta = \nabla \cdot \nabla$ and "$\cdot$" stands for the tensor multiplication (with one repeated index if indicial notation is used). The time derivative in (1) is

partial, as a consequence of the simplifying assumptions, however, usually even this term is neglected and the filling process is taken as steady state (at each time stage). Fibers are assumed impermeable, rigid and with perfectly fixed location. The resin surface tension and the air pressure can be neglected and then the boundary conditions have forms ([4]):

$$\begin{aligned} &\text{at the resin front: } \partial f/\partial t+\mathbf{v}\cdot\nabla f=0,\ \boldsymbol{\sigma}\cdot\mathbf{n}=\mathbf{0},\\ &\text{at the mold walls and the fiber boundary: } \mathbf{v}=\mathbf{0},\\ &\text{at the injection gates: } \mathbf{v}=\mathbf{v}_0 \text{ or } p=p_0, \end{aligned} \tag{2}$$

where $\mathbf{n}$ is the unit normal vector to corresponding surfaces, $\boldsymbol{\sigma}$ is the stress tensor and subscript 0 refers to the imposed values. The function $f(\mathbf{x}(t),t)=0$ describes the moving front position.

Micro and macrolevel problems equivalent to (1-2) can be formulated exploiting either asymptotic expansion ([5-8]) or local averaging ([8]) methods. It turns out, that the macrolevel problem is, in fact, the well-known Darcy's law for incompressible flows through porous media:

$$\nabla\cdot\mathbf{v}^D=0 \text{ and } \mathbf{v}^D=-(\mathbf{K}\cdot\nabla P)/\mu, \tag{3}$$

where the first relation is the macroscopic equation of the homogenization theory corresponding to the continuity equation inside the saturated regions, $\mathbf{v}^D$ is the vector of the Darcean velocity, P is the macroscopic pressure and volume forces were neglected; $\mathbf{K}$ stands for the permeability tensor and has to be determined from a microlevel problem. Both, $\mathbf{v}^D$ and P, are obtained from the microscopic values, $\mathbf{v}$ and p, by averaging, i.e. $\mathbf{v}^D=\langle v\rangle$ and $P=\langle p\rangle$, where $\langle.\rangle$ is the averaging operator. The boundary conditions for the macrolevel problem are:

$$\begin{aligned} &\text{at the resin front: } \partial f/\partial t+(\mathbf{v}^D\cdot\nabla f)/\phi=0,\ P=0,\\ &\text{at the mold walls: } \partial P/\partial n=0,\\ &\text{at the injection gates: } \mathbf{v}^D=\langle\langle\mathbf{v}_0\rangle\rangle \text{ or } P=\langle\langle P_0\rangle\rangle, \end{aligned} \tag{4}$$

where ϕ is the porosity and $\langle\langle.\rangle\rangle$ stands for the area average at the injection gates.

For periodic preforms, the asymptotic expansion method can be used to formulate the microlevel problem ([5-8]). The first non-zero term in the asymptotic expansion of the velocity vector (for the sake of simplicity with the square of the small parameter included), $\mathbf{v}^{(0)}$, is given by:

$$\mathbf{v}^{(0)}=\frac{\chi^m}{\mu}\left(F_m-\frac{\partial p^{(0)}}{\partial x_m}\right),$$

where χ^m is a characteristic solution of the microscopic equation of the homogenization theory, fulfilling $K_{im}=\langle\chi_i^m\rangle$. $p^{(0)}$ is the first non-zero term from the pressure expansion and $\mathbf{v}^D=\langle v^{(0)}\rangle$ and $P=\langle p^{(0)}\rangle$. χ^m is, in fact, the velocity vector related to Stokes flow of the unit-viscosity liquid in the (fully filled) basic cell, if either negative unit macro-pressure gradient or positive unit macro-volume force in direction m is applied on the basic cell. Periodicity boundary conditions must be imposed on χ^m components and on the pressure or on the pressure reduced by the value corresponding to the applied gradient. The main advantage of the microlevel problem is that the problem is linear and the permeability tensor depends only on the geometry of the fiber mats.

3 MICROLEVEL ANALYSIS

The numerical calculation of the permeability tensor is still not very common and values obtained from experimental measurements are usually introduced into the macrolevel problem. However, ANSYS preprocessor and ANSYS Parametric Design Language permit an easy generation of complicated geometries and the numerical determination of permeability values is relatively easy.

Since Stokes flow in a fully saturated basic cell has to be solved, the well-known analogy with incompressible elasticity can be used ([9]). Continuity equation can be satisfied by introduction of the Poisson's ratio of the related elastic material, ν^r, very close to 0.5. Periodicity conditions can only be imposed on the boundary displacements, since due to the variational formulation of the problem, they enforce the periodicity of the boundary pressure, thus it is easier to prescribe the unit macro-volume force than the pressure gradient. Permeability values for perpendicular flow across aligned circular fibers with in-line arrangement were calculated and compared with numerical results from [5], [8] and [10]. In calculations no hybrid formulation was used and only small variations in the pressure values and no variations in the velocity (displacement) values for different (close to 0.5) ν^r were obtained. The permeability results are acceptable already for ν^r=0.4999 ([11]). In addition, recirculation regions can easily be detected from the results.

When the problem of double porosity (if fibers are in fact fiber-tows consisting of several fibrils, [5], [10]) is addressed, several approaches are possible. E.g. the cell-averaged permeability, ${}^c\mathbf{K}$, can be calculated ([10]) or the macrolevel problem can be solved in two levels ([5]), exploiting the intra-tow permeability, ${}^t\mathbf{K}$ (within the fiber-tows), and the inter-tow permeability, ${}^i\mathbf{K}$ (the fiber-tows are assumed as full), etc. ${}^c\mathbf{K}$ can be calculated directly in the same way as the single porosity permeability, only all the single fibrils constituting the fiber-tows have to be modeled in the basic cell. For the perpendicular flow across aligned circular fiber-tows it was concluded in [10], that a significant increase of ${}^c\mathbf{K}$ with respect to ${}^i\mathbf{K}$ occurs for $\phi_i<0.4\phi_t$, where ϕ_i and ϕ_t stand for the intra-tow and the inter-tow porosity, respectively.

On the other hand, a representative permeability, ${}^r\mathbf{K}$, of a specimen with n fiber-tows (Fig. 1, no dependence on the direction along the fiber-tows), determined by solving the macrolevel problem in two levels, exhibits different properties. Let us estimate the filling time in this case. When constant volume rate is imposed at the injection gate, then the filling time depends only on the porosity. When the inlet pressure, P_0, is applied, the filling time t^D of one-dimensional specimen of length D and longitudinal permeability K and the filling time t^R of a circular fiber tow with radius R_t, surrounding pressure P_t and radial permeability K can be calculated from:

$$t^D=\frac{\mu\phi D^2}{2KP_0} \text{ and } t^R=\frac{\mu\phi R_t^2}{4KP_t},$$

respectively. Summing up:

$$\frac{\phi D^2}{{}^rKP_0}=\frac{\phi_i D^2}{{}^iKP_0}+\sum_{k=1}^{n}\frac{\phi_t R_t^2}{2^tKP_{t,k}},$$

where ${}^rK$, ${}^iK$ stand for the representative and intra-tow longitudinal permeability, respectively, and ${}^tK$ stands for the radial inter-tow permeability. It can be assumed that the filling of the fiber-tows is directed by the pressure surrounding the fibers $P_{t,k}=P_0(k-1/2)/n$, yielding

$$\frac{\phi}{{}^rK}=\frac{\phi_i}{{}^iK}+\frac{\phi_t R_t^2 n}{2^tKD^2}\sum_{k=1}^{n}\frac{1}{k-1/2}, \qquad (5)$$

where obviously

$$\frac{R_t^2}{D^2}=\frac{1-\phi_t}{\pi n^2} \text{ and } \phi=1-(1-\phi_i)(1-\phi_t).$$

Let us take D=1. ${}^iK$ and ${}^tK$ can be introduced into (5) in their analytical form from [12] (for simplicity no hybrid model, but only junction of lubrication (for porosities less than 0.55) and cell method results (for reminding porosities) was used). Adopting $r_f^2=(1-\phi_i)(1-\phi_t)/(\pi mn^2)$, where

r_f is the radius of a single fibril and m is the number of fibrils in a fiber-tow, the dimensionless representative permeability ${}^{r}Kn^2$ can be expressed from (5) as a function of ϕ_i, ϕ_t, n and m. ${}^{i}Kn^2$ (full line) is compared with ${}^{r}Kn^2$ for different ϕ_t (dashed lines) in Fig. 2. The curves (n=100 and m=100) are plotted in logarithmic scale and with respect to ϕ_i. It is seen that the significant decrease of ${}^{r}Kn^2$ with respect to ${}^{i}Kn^2$ occurs especially for low ϕ_t.

It is thus obvious, that to the double porosity problem must be paid a special attention. Furthermore, the permeability calculation assumes fully filled basic cells, however, the void formation is originated at the microlevel. Due to these two facts, it is worthwhile to study the progression of the resin front at the microlevel. With this purpose an algorithm suited for ANSYS (exploiting the ANSYS Parametric Design Language) was developed, so far only for 2D problems. The new resin front position is calculated directly using the free boundary condition. At time stage $t=t_k$ the front shape is approximated locally by a circle at each nodal point (using two adjacent points) and a local coordinate system is introduced at this nodal point with axes in normal (x_n) and tangential (x_t) directions to the front. Then, for $x_n=g(x_t)$ being the front equation in the local coordinate system, it follows from the free boundary condition, that:

$$v_n - v_t \frac{\partial g}{\partial x_t} = v_n = \frac{\partial g}{\partial t}.$$

If backward difference method is used for the time derivative, then simply:

$$x_{n,t_{k+1}} = x_{n,t_k} + (t_{k+1} - t_k) v_n \qquad (6)$$

at $t=t_{k+1}$. At each time stage it is thus necessary to solve the linear analogous problem and then the algorithm generates and remeshes the new filled domain exploiting the new nodal points positions from (6). Therefore, the algorithm is stable and not time-consuming.

The algorithm was verified on the example of Stokes flow between two rigid plates for a parabolic and a uniform inlet velocity profile. The parabolic velocity profile was maintained while the uniform one was transformed along the specimen to the parabolic one (Fig 3-4). The flow front shape was stabilized in both cases on the same shape (Fig. 4); results thus coincide with the theoretical predictions. The resin front progression was then studied in the basic cell of a perpendicular flow across aligned circular fibers with in-line arrangement (ϕ=0.804), velocity profile corresponding to the steady-state situation of the fully filled cell was imposed on the left part of the cell. Results are plotted in Figs. 5-6 for different time stages, corresponding to one of the initial stages, to the stage when the resin front touches the fiber, when the front part is fully filled and when the upper part of the front reaches the end of the cell. In this stage it is seen, that the part behind the fiber is not yet filled, but the velocity distribution resembles the steady-state situation in the fully filled basic cell.

Non-linear effects can be introduced into the algorithm by generalization of the analogous problem (linear incompressible elastic problem), but then each time stage would require a non-linear analysis. Central difference algorithm for the time derivative could be also implemented. Moreover, the algorithm can also be used for the purposes of the macrolevel analysis.

4 MACROLEVEL ANALYSIS

Problem (3) can be reformulated. The equation $\nabla \cdot \mathbf{v}^D = 0$, valid inside saturated regions, can be extended to a form derived e.g. in [13], which allows for a direct determination of the front position at each time step. Then the Darcy's analysis resembles the heat transfer analysis ([14]):

$$\gamma\left(\phi(\mathbf{x})\frac{\partial}{\partial t}s(\mathbf{x},t)+\nabla\cdot\mathbf{v}^{D}(\mathbf{x},t)\right)=0, \qquad \rho_c\frac{\partial}{\partial t}U(\mathbf{x},t)+\nabla\cdot\mathbf{q}(\mathbf{x},t)=0,$$

$$\mathbf{v}^{D}(\mathbf{x},t)=-(\mathbf{K}(\mathbf{x})\cdot\nabla P(\mathbf{x},t))/\mu, \qquad \mathbf{q}(\mathbf{x},t)=-\mathbf{T}(\mathbf{x})\cdot\nabla\Theta(\mathbf{x},t).$$

γ and s, denote the resin specific weight and the saturation in the porous medium; ρ_c, U, $\mathbf{q}$, $\mathbf{T}$ and Θ stand for the density, internal energy, heat flux vector, thermal conductivity tensor and the temperature, respectively. The boundary conditions (4) do not have to be reformulated, only the free boundary condition can be omitted.

Since the saturation, s, is restricted to the interval [0,1], the same kind of restriction must be ensured in the analogous (heat transfer) problem, thus U must always belongs to the interval $[0,\phi]$. A fictitious medium has to be introduced, as it is described in [11]. The relation ([13])

$$\frac{\partial}{\partial t}U(\mathbf{x},t)=c(\mathbf{x},t)\frac{\partial}{\partial t}\Theta(\mathbf{x},t), \text{ where } c(\mathbf{x},t)=\frac{d}{d\Theta}U(\Theta(\mathbf{x},t))$$

can be exploited (c being the specific heat) at this point. Furthermore, a front region with finite width has to be defined. Under assumption of linear "heat gaining", c is piece-wise constant with two different values, non-zero ($c=c_0$) and zero ($c=0$) defining like that two regions. They are: the region where the fictitious medium is not yet "fully saturated" (including the front region, where the medium already started to gain heat) and the region where the medium is already "fully saturated". In order to model such situation, an initial temperature, Θ_i must be introduced in the fictitious medium, and a temperature, Θ_s, that will correspond to the "saturated state" has to be stated. It holds $\phi(\mathbf{x})=(\Theta_s-\Theta_i)\,c_0(\mathbf{x})$ and the front region is characterized by $\Theta\in(\Theta_i,\Theta_s]$. The central difference method is necessary to use in the numerical solution, due to the discontinuity in the time derivative of the internal energy.

The main advantage of the approach proposed above is that the position of the resin front is solved directly and that the FE code ANSYS can be used in the RTM filling-phase simulation, bringing large variety of the FE and a powerful postprocessor allowing good visualization of the results. Progression of the resin front in example described in [15], whose results are compared there with experimental measurements, is plotted in Fig. 7, together with the FE mesh and isobars for t=105s (characteristic dimensions of the mold are 1m and 0.5m, ϕ=0.89, K/μ=3.41e-8 m^3s/kg and the inlet flow rate is 3.14e-3 m^2/s). The numerical saturated area is compared in Fig. 8 with the analytical prediction. Front progression in orthotropic preforms is plotted in Fig. 9 for the ratio of the principal permeabilities $K_{22}/K_{11}=2$. The ratio of the principal ellipsoid axes exhibit excellent coincidence with theoretically predicted $\sqrt{2}$ ([14]).

5 MULTIPLE-LAYER PREFORMS

Typical specimens are relatively thin, allowing the macrolevel problem to be stated only on a two-dimensional surface. However, fiber mats consist of various (macroscopically homogeneous) layers, stacked together, whose directional properties are usually very different. In order to restrict the analysis to a two-dimensional surface, another homogenization step must be done in the transversal (thickness) direction, yielding a thickness-homogenized permeability $^{H}\mathbf{K}$.
The analytical solution of $^{H}\mathbf{K}$ on a fully saturated layered basic cell, under periodicity boundary conditions results in $^{H}\mathbf{K}=^{A}\mathbf{K}$, where $^{A}\mathbf{K}$ is the thickness-averaged permeability. However, in [16] the difference between the unsaturated ($^{HR}\mathbf{K}$) and saturated ($^{A}\mathbf{K}$) in-plane permeability is verified experimentally and in [17-18] analytical determination of $^{HR}\mathbf{K}$ is presented.

In [11] the calculation of non-uniform front characteristics is proposed differently than in [17-18]. The correctness of ${}^{H}\mathbf{K}={}^{A}\mathbf{K}$ is justified in the sense, that if theoretical predictions of the flow front position are required, ${}^{A}\mathbf{K}$ and characteristics of the non-uniformity calculated using the approach proposed in [11] are sufficient. Two regions: the homogenized region and the transition region, where the transversal flow is trying to equilibrate the flow into the homogenized state, can be distinguished in the layered specimen. Let us restrict ourselves to a two-layer specimen (no dependence on one of the layer direction) with equal thicknesses and constant porosity.

In the homogenized region the flow takes place only in layers direction with constant but different velocity in each layer (Fig. 10). The pressure is independent on the transversal direction (Fig. 11), thus the ratio of the resin velocities in layer 1 (${}^{1}v^{H}$) and in layer 2 (${}^{2}v^{H}$) is $\frac{{}^{1}v^{H}}{{}^{2}v^{H}}=\frac{{}^{1}K}{{}^{2}K}$ justifying that the homogenized region is sufficiently described by ${}^{A}\mathbf{K}$.

The characteristics of the transition region, ${}^{L}d$, ${}^{1}d$, ${}^{2}d$ (the notation is specified in Fig. 11) and so the flow front difference, ${}^{2}d$-${}^{1}d$, do not depend on the distance from the injection gate, consequently do not depend on the transition pressure, P_{tr}, which is defined as the pressure on the interface between the two regions. The pressure distribution at middle axes of layer 1 and 2, ${}^{1}P(x)$ and ${}^{2}P(x)$, can be approximated as piece-wise linear with different slopes in the homogenized and transition regions (Fig. 11, ${}^{L}P(x)$ and ${}^{H}P(x)$ stand for the pressure distribution at middle axes of the layered and the homogenized specimens, respectively). ${}^{L}d={}^{H}d$, while $({}^{1}d+{}^{2}d)/2\neq{}^{L}d$. In the calculation of the transition region characteristics it is assumed that if the homogenous region is removed and the filling process starts from the prescribed transition pressure, P_{tr}, then it takes time, t_{tr}, to fully form the transition region. The mass balance ([17-18]) can be written (${}^{1}K<{}^{2}K$) as:

$$ {}^{1}v+{}^{21}v={}^{2}v-{}^{21}v, \tag{7}$$

where ${}^{1}v$, ${}^{2}v$ and ${}^{21}v$ are the volume rates in the transition region longitudinally in layer 1, in layer 2 and in direction from layer 2 into layer 1, respectively. The pressure gradient originating ${}^{21}v$ can be expressed in terms of the area of the pressure difference, ${}^{2}P(x)$-${}^{1}P(x)$, which is $P_{tr}\left({}^{2}d(t)-{}^{1}d(t)\right)/2$. Then:

$${}^{1}v(t)={}^{1}K\frac{P_{tr}h}{{}^{1}d(t)\mu},\ {}^{2}v(t)={}^{2}K\frac{P_{tr}h}{{}^{2}d(t)\mu}\ \text{and}\ {}^{21}v(t)={}^{T}K\frac{\left({}^{2}d(t)-{}^{1}d(t)\right)P_{tr}}{2\mu h}.$$

Total volumes of the flowing resin can be calculated by time integration over the interval $[0, t_{tr}]$:

$${}^{1}V={}^{1}K\frac{2P_{tr}ht_{tr}}{{}^{1}d\mu},\ {}^{2}V={}^{2}K\frac{2P_{tr}ht_{tr}}{{}^{2}d\mu}\ \text{and}\ {}^{21}V=\frac{\left({}^{2}d-{}^{1}d\right)P_{tr}t_{tr}{}^{T}K}{3\mu h},$$

where for the sake of simplicity ${}^{1}d={}^{1}d(t_{tr})$ and ${}^{2}d={}^{2}d(t_{tr})$ is used. It must hold:

$$ {}^{1}V+{}^{21}V={}^{1}dh\phi\ \text{and}\ {}^{2}V-{}^{21}V={}^{2}dh\phi. \tag{8}$$

(7-8) with $t=t_{tr}$ substituted form the basic equations to be solved. The solution is:

$$P_{tr}t_{tr}=\frac{3\phi\mu h^{2}}{4{}^{T}K},\ {}^{1}d=\frac{h}{2\sqrt{10}}\sqrt{\frac{{}^{2}K+49{}^{1}K+\sqrt{{}^{2}K^{2}+98{}^{2}K{}^{1}K+{}^{1}K^{2}}}{{}^{T}K}}\ \text{and}$$

$${}^{2}d=\frac{5h}{2\sqrt{10}}\frac{{}^{2}K+{}^{1}K+\sqrt{{}^{2}K^{2}+98{}^{2}K{}^{1}K+{}^{1}K^{2}}}{\sqrt{{}^{T}K\left({}^{2}K+49{}^{1}K+\sqrt{{}^{2}K^{2}+98{}^{2}K{}^{1}K+{}^{1}K^{2}}\right)}}. \tag{9}$$

Let time t_0 be given, then the resting non-uniform characteristics corresponding to this time are:

$$P_{tr} = h\sqrt{\frac{3\phi\mu P_0}{4^T K t_0}},\quad t_{tr} = P_{tr}\frac{t_0}{P_0},\quad {}^L L = {}^H L = \sqrt{\frac{2^A K P_0 t_0}{\phi\mu}} \text{ and } {}^H D = {}^H L\left(1 - \frac{P_{tr}}{P_0}\right).$$

In Fig. 12 the numerical dimensionless flow front difference $({}^2d - {}^1d)/H$ from comparative example with ${}^T K/\mu = 10\ m^3 s/kg$, ${}^1K/\mu = 2\ m^3 s/kg$, ${}^2K/\mu = 8\ m^3 s/kg$, $P_0 = 5e\text{-}5(Pa)$, $\phi = 0.5$ and $h = H/2 = 0.05m$ is compared with the results from [17-18] and formula (9), plotted with respect to ${}^1L/H$ (${}^1L$ being the total saturated length in layer 1). It is seen that the coincidence of (9) with the numerical results is very good; the error increases with the difference between ${}^1K$ and ${}^2K$.

6 CONCLUSION

In this paper the utilization of general-purpose commercial FE codes, particularly ANSYS, is demonstrated. The utilization is made possible by stating an analogy between Stokes flow and incompressible elasticity and between Darcy's problem with moving boundary and transient heat transfer problem. Moreover, an algorithm allowing determination of the resin front position at microlevel is developed, which will be used in studying of some particular problems, especially of the double porosity problem. On the other hand, the approach to the progression of the resin front and very good visualization of the results at macrolevel was utilized in the study of multi-layer preforms.

REFERENCES

[1] *ANSYS Analysis Guides*, 1th Edition, Swanson Analysis Systems IP, Inc., Version 5.3, 1997.

[2] *ANSYS Commands Reference*, 7th Edition, Swanson Analysis Systems IP, Inc., Version 5.3, 1997.

[3] *ANSYS Theory Reference*, 7th Edition, Swanson Analysis Systems IP, Inc., Version 5.3, 1997.

[4] White, F.M., *Fluid Mechanics*, McGraw-Hill, Inc., 1994, pp. 192-242.

[5] Chang, W., *Modeling and Numerical Analysis of Composite Manufacturing Processes*, Ph.D. Dissertation, The University of Michigan, 1993.

[6] Sanchez-Palencia, E., *Non-Homogeneous Media and Vibration Theory*, Lecture Notes in Physics, **127**, Springer-Verlag, 1980, pp.129-157.

[7] Ene, H.I. and Polisevski, D., *Thermal Flow in Porous Media*, D. Reidel Publishing Company, 1987, pp. 1-47.

[8] Kaviany, M., *Principles of Heat Transfer in Porous Media*, Springer-Verlag New York, Inc., 1995, pp. 15-118.

[9] Hughes, T.J.R., *The Finite Element Method. Linear Static and Dynamic Finite Element Analysis*, Prentice-Hall International, Inc., 1987, pp. 192-217.

[10] Papathanasiou, T.D., A structure oriented micromechanical model for viscous flow through square arrays of fibre clusters, *Composites Science and Technology*, 1996, **56**, 1055-1069.

[11] Dimitrovová, Z. and Faria, L., Finite element modeling of the resin transfer molding process based on homogenization techniques, *Computers & Structures*, accepted.

[12] Bruschke, M.V. and Advani, S.G., Flow of generalized Newtonian fluids across a periodic array of cylinders, *Journal of Rheology*, 1993, **37**, 479-498.

[13] *Abaqus/Standard Theory Manual*, Hibbitt, Karlsson and Sorensen, Inc., Version 5.6, 1998.

[14] Carslaw, H.S. and Jaeger, J.C., *Conduction of Heat in Solids*, Oxford Science Publications, Clarendon Press, Oxford, 1959, pp. 1-49.

[15] Trochu, F., Gauvin, R. and Gao, D.-M., Numerical analysis of the resin transfer molding process by the finite element method, *Advances in Polymer Technology*, 1993, **12**, 329-342.

[16] Luce, T.L., Advani, S.G., Howard, J.G. and Parnas, R.S., Permeability characterization. Part 2: Flow behavior in multiple-layer preforms, *Polymer Composites*, 1995, **16**, 446-458.
[17] Bruschke, M.V., Luce, T.L. and Advani, S.G., Effective in-plane permeability of multi-layered RTM preforms, *Proc. of 7th Tech. Conf. on Composite Materials*, American Society for Composites, 1992, pp. 103-112.
[18] Calado, V.M.C. and Advani, S.G., Effective averaged permeability of multi-layer preforms in resin transfer molding, *Composites Science and Technology*, 1996, **56**, 519-531.

FIGURES

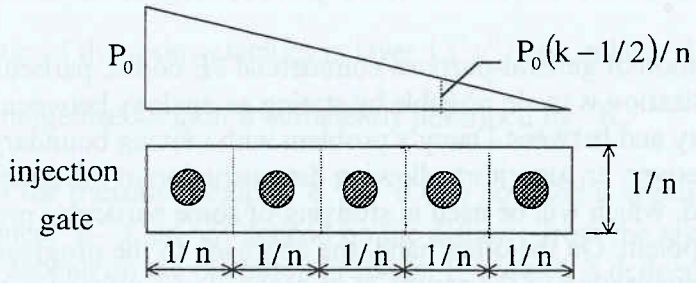

Fig. 1 – The specimen with n fiber-tows used in determination of the representative permeability ^{r}K

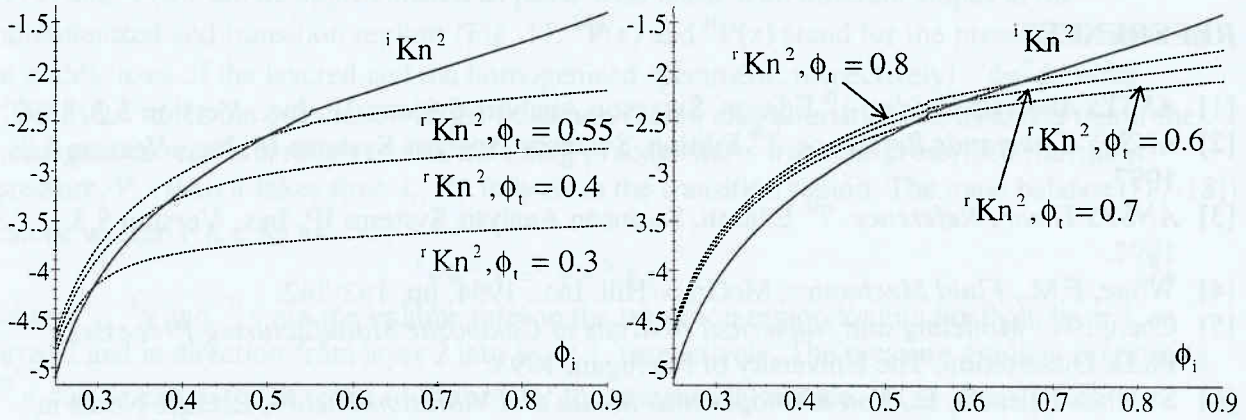

Fig. 2 – Comparison of $^{i}Kn^{2}$ with $^{r}Kn^{2}$ for various ϕ_t={0.3, 0.4, 0.55, 06, 0.7, 0.8} of the specimen from Fig. 1

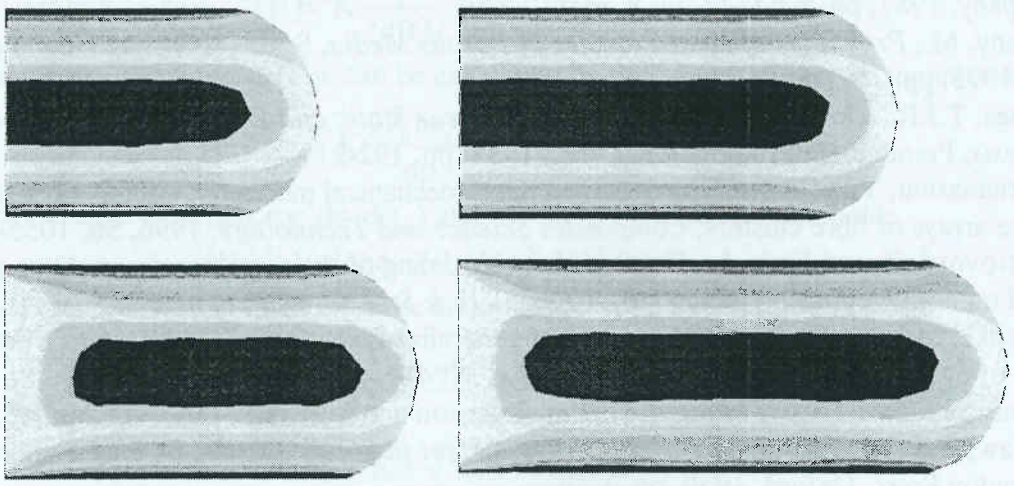

Fig. 3 – Stokes flow between two rigid plates, parabolic inlet velocity profile (above) and uniform inlet velocity profile (below)

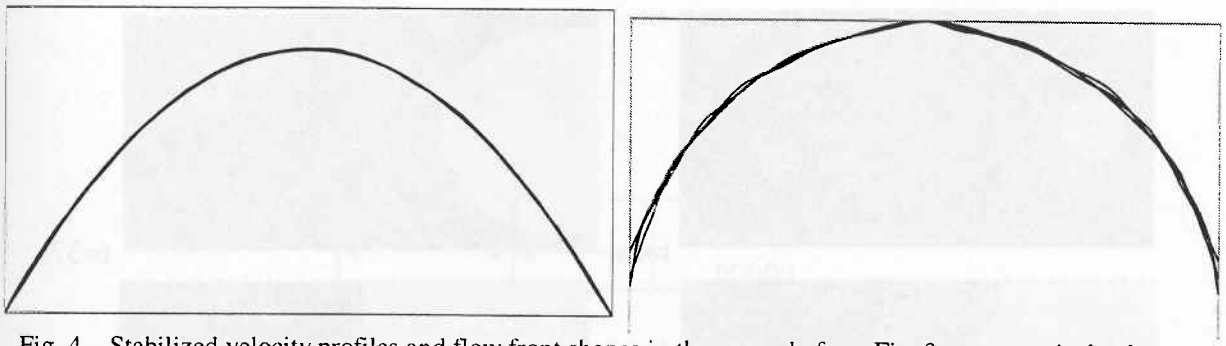

Fig. 4 – Stabilized velocity profiles and flow front shapes in the example from Fig. 3, no numerical values are shown, since this is only a comparative example

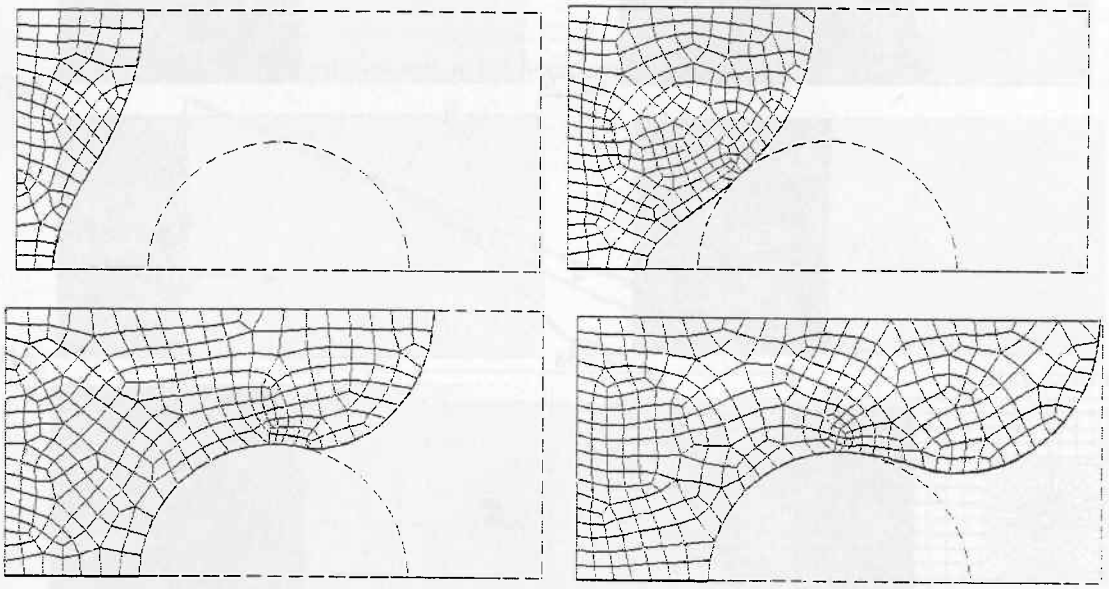

Fig. 5 – Resin front progression in the basic cell of perpendicular flow across aligned circular fibers

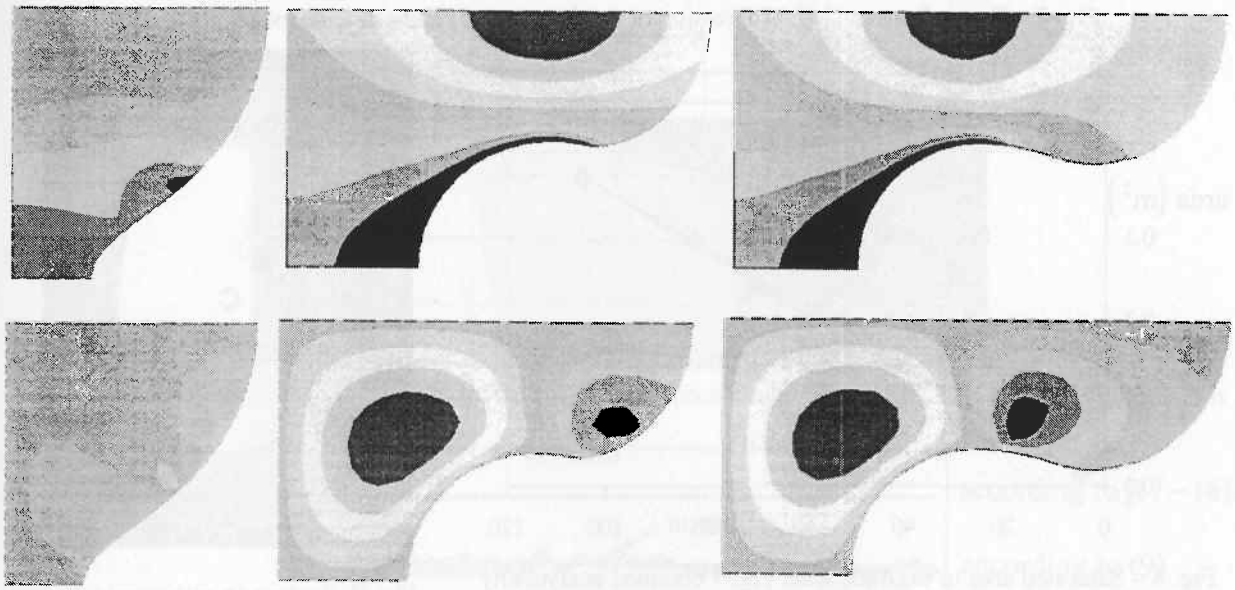

Fig. 6 – Horizontal (above) and vertical (below) components of velocity in last three stages from Fig. 5 (no numerical values are shown, since this is only a comparative example)

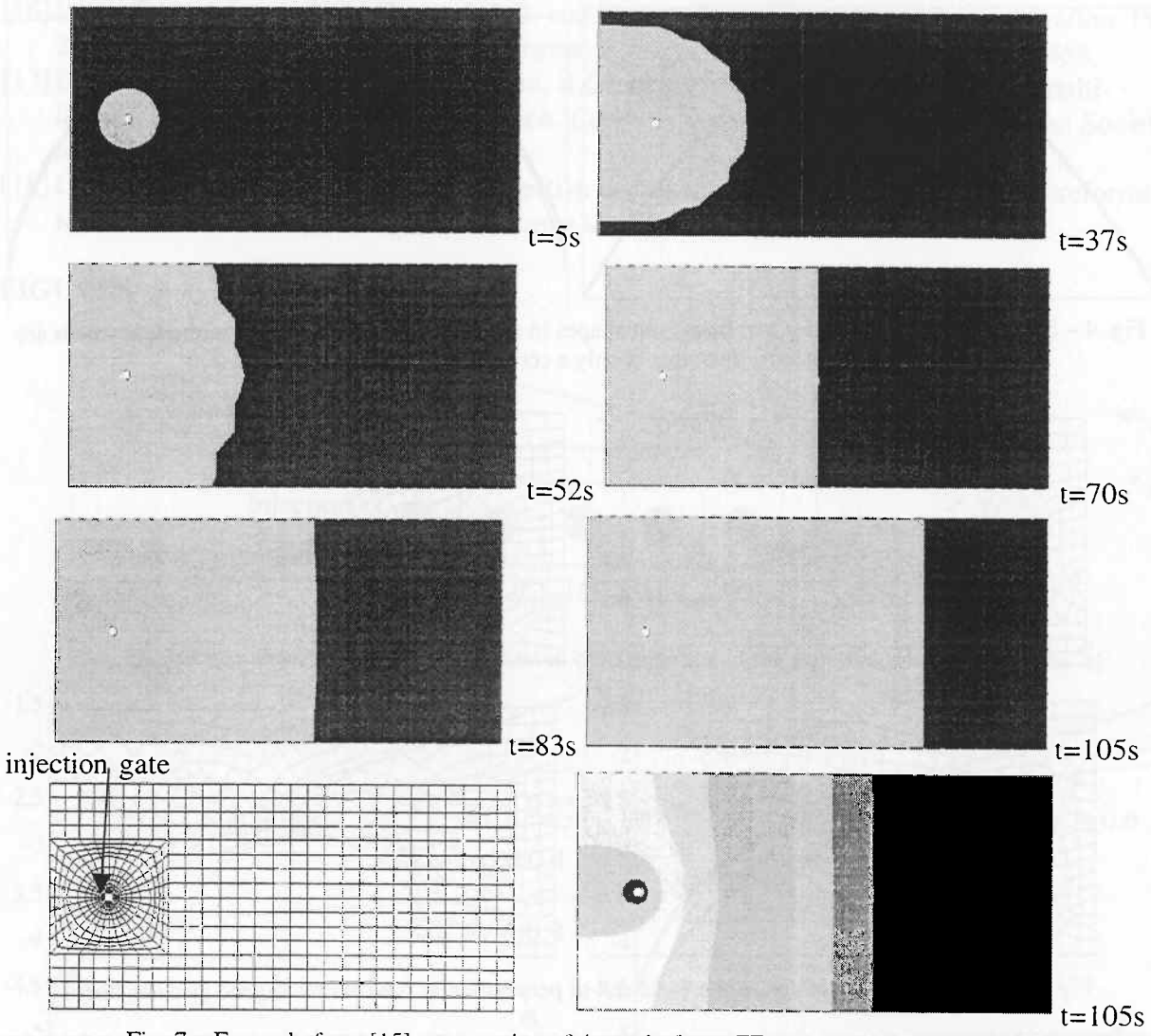

Fig. 7 – Example from [15], progression of the resin front, FE mesh and isobars at t=105s

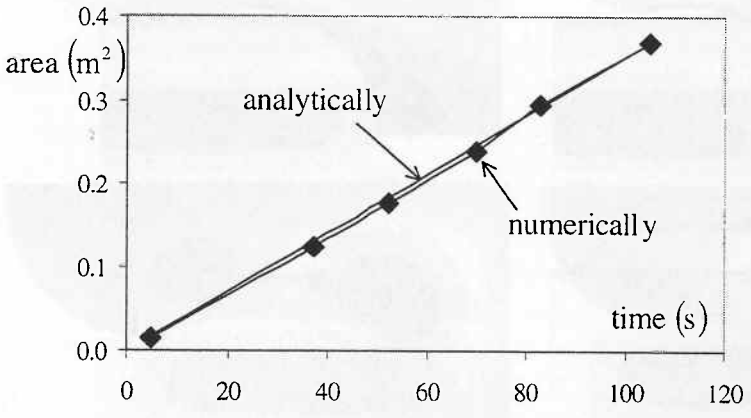

Fig. 8 – Saturated area in example from Fig. 7 obtained analytically and numerically

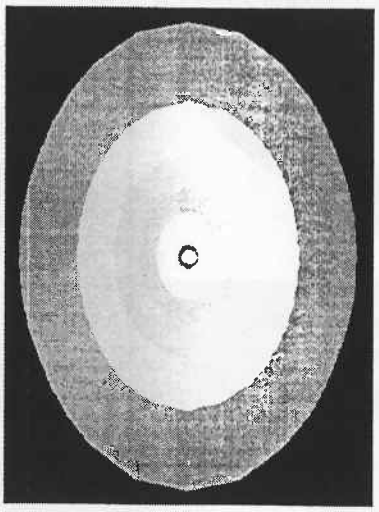

Fig. 9 - Isobars in orthotropic preform

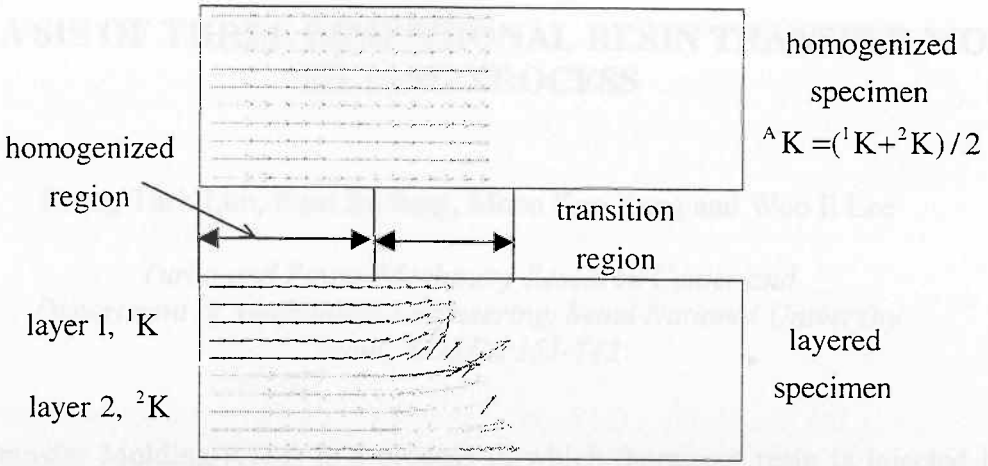

Fig. 10 – Resin velocity in the homogenized and transition regions

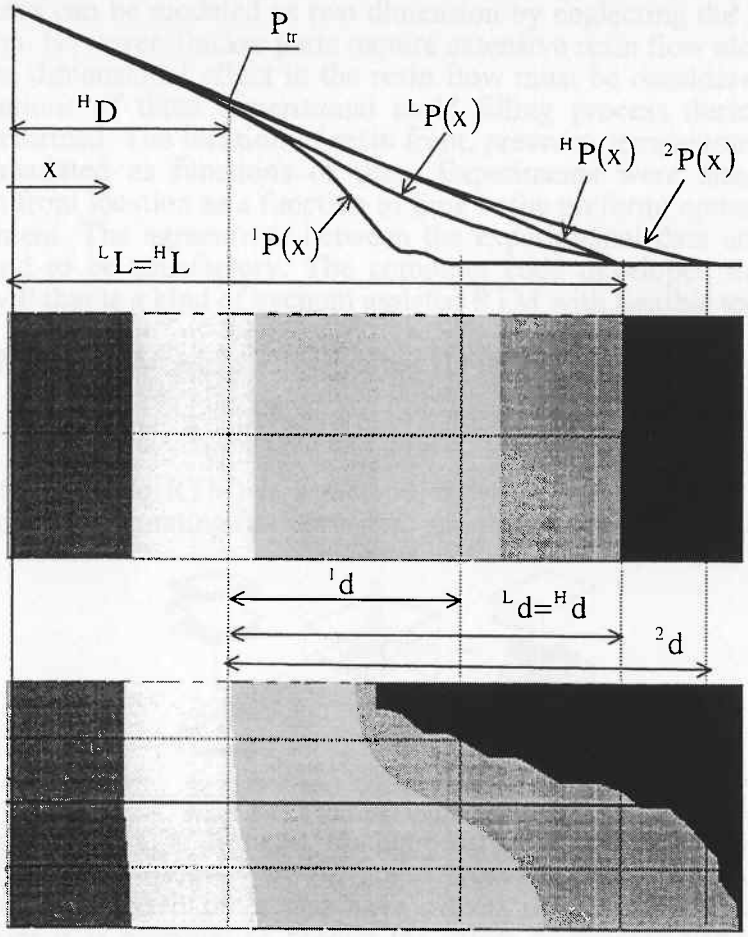

Fig. 11 – Pressure distribution along the specimens and the specification of homogenized and transition regions

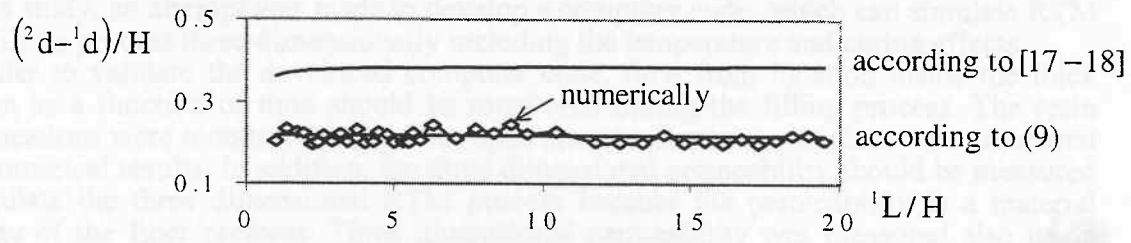

Fig. 12 – Flow front difference obtained numerically and analytically in the comparative example